Two dimensional direct numerical simulation of nonreacting confined supersonic mixing layer

D. Chakraborty
Aerodynamics Division, Vikram Sarabhai Space Centre
Thiruvananthapuram, India

H. S. Mukunda and P. J. Paul
Department of Aerospace Engineering
Indian Institute of Science, Bangalore, India

ABSTRACT

Direct Numerical Simulation (DNS) results are presented for high speed nonreacting mixing layer in a confined test section. The hypervelocity mixing layer experiment of Erdos *et al* with H_2/N_2 stream is simulated by discretizing two dimensional Navier Stokes equation using a higher order (fourth order spatial and second order temporal) compact numerical algorithm. A favourable comparison of the computation with experimentally measured wall static pressure forms the basis of further analysis. Instantaneous flow picture and the mean profiles of various flow variables were examined to determine the development and general characteristics of the confined mixing layer. It has been found that the growth of the mixing layer is towards the high speed side of the layer. Various turbulence quantities were derived from the stored time series data of the DNS calculation and the results were compared with the experimental results of supersonic free shear layer as no experimental results of turbulence statistics are available for the confined hypervelocity mixing layer. The increasing Reynolds stress data with the flow direction indicate that the turbulence is sustained by transferring the energy from the mean flow to the fluctuating field as the shear layer develops. Although the Reynolds stress is negligible in the most portion of the wall boundary layers, effect of counter gradient effect is observed in the far downstream location of the lower wall boundary layer. The general conclusion that for the supersonic mixing layer, various turbulence quantities like Reynolds stress, turbulence intensities (both streamwise and transverse) decrease with the increase in the convective Mach number is also confirmed by our results.

1.0 INTRODUCTION

High Mach number mixing layers play an important role in the development of supersonic combustor ramjet (Scramjet) engines. Supersonic mixing layer is inherently more stable than its subsonic counterpart and this results in the practical consequence that there is less mixing. For the scramjet propulsion device, where chemical reaction and heat release occur in the supersonic streams of fuel and air, adequate mixing between fuel and air is an essential requirement. The physics behind compressible mixing between two streams is still poorly understood.

Non-reacting supersonic free shear layers are investigated for the last few decades by experiment[1-6], stability analysis[7,8] and numerical analysis[9,10]. The major results and issues on the non-reacting free shear layers are discussed extensively in many review articles[11,12]. The precise reasons for the reduced growth rate with increasing convective Mach number are yet elusive.

Adequate attention has not been received in the literature in the analysis of laterally confined supersonic shear layer. There exists a fundamental difference in the development of turbulence in the wall boundary layer and the mixing layer. The interaction between the two can affect the structure of the flow and the growth rate of the mixing layer significantly. Experimental studies onconfined shear layer are not many. One important experiment on hypervelocity mixing layer is the work of Erdos *et al*[13] in which gaseous H_2 and N_2 at Mach numbers of 3·09 and 3·99 flow off a splitter plate in a 25·4mm high rectangular test section of more than 500mm length. Measurements are limited to wall static pressures and heat flux. Flow visualization using laser holographic interferometry and pictures of schlieren and shadowgraph as well as finite and infinite fringe interferometry have been presented. Although the measurements of turbulence quantities of supersonic free mixing layer are reported in a few studies[2,3,14,15], no results have been reported on the turbulence measurements in confined supersonic mixing layer.

A few studies on the numerical simulation of the confined supersonic mixing layer are reported in the literature. Guirguis *et al*[16] and Faruk *et al*[17] performed two dimensional inviscid simulation to determine the evolution of the shear layer formed by two parallel streams of air in a confined environment. The velocities, densities and the static pressures of the two streams are varied in these studies to determine the effect of these parameters on the growth of the mixing layer. Lu and Wu[18] has also performed numerical investigation of non-reacting supersonic confined mixing layer by solving two dimensional Euler equations to study the effect of shock in the mix-

Paper No. 2523. Manuscript received 4 January 2000, 1st revision received 31 May 2000, accepted 22 June 2000.

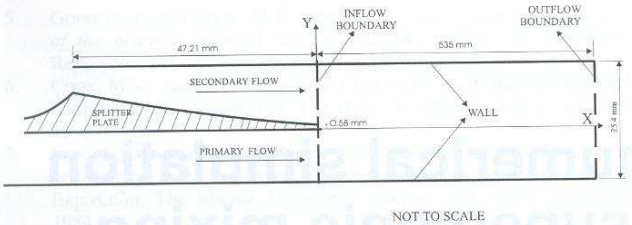

Figure 1. Schematic of the experimental setup[13] for which computations have been made.

ing enhancement process and concluded that the shock induced mixing improvement is local around the shock-impingement area. As these simulations are inviscid in nature, the viscous phenomena, particularly the effect of wall boundary layers on the growth and structure of the mixing layer have not been addressed.

In this paper, we will investigate the non-reacting confined mixing layer experiment of Erdos *et al*[13] through Direct Numerical Simulation (DNS). The cleanliness of the geometry, adequate test section length for the flow to develop and the measured wall pressures provide enough incentive to examine through computational technique this hypervelocity experiment. The stored time series data of DNS is also analyzed to obtain the turbulent statistics of the confined supersonic mixing layer.

2.0 CONSIDERATIONS FOR SIMULATION

The present model free simulation deals with only H_2/N_2 case, although the experimental investigation of Erdos *et al*[13] consists of two different non-reacting cases namely mixing of H_2/N_2 and N_2/N_2 streams.

In the simulation, the N_2 stream is considered as the primary (lower) flow with Mach 3·99 and separated by a splitter plate from the H_2 stream with Mach 3·09 which is considered as the secondary stream (upper). The schematic of the experimental setup[13] for which the computations are made is shown in Fig. 1 along with the computational boundaries. The details of the flow parameters for the test conditions are presented in Table 1. The convective velocity is 3,000 m/sec and the convective Mach numbers are 0·85 and 0·82 referred to as H_2 and N_2 streams, respectively.

Although the free shear layer experimental studies of Clemens and Mungal[5], Elliott *et al*[6] and the linear stability analysis[7,8] suggest that oblique disturbances become more and more unstable as convective Mach number exceeds 0·6 and three dimensional effect becomes more predominant. But, Tam and Hu[19] point out through their linear instability analysis of the confined supersonic mixing layer that there exists a new instability mechanism called 'Supersonic Instability' arising from the coupling between the motion of the shear layer and the reflected channel acoustic wave. The 'Supersonic Instability' is different from the classical 'Kelvin-Helmholtz' instability associated with subsonic free shear flows. The existence of 'Supersonic instability' is also reported from the linear stability analysis of confined temporal supersonic mixing layers by Greengough *et al*[20]. Zhaung *et al*[21] confirmed Tam and Hu's conclusion and showed that the disturbance waves propagate outwards from the shear layer along the Mach angle and the confined walls provide a 'feedback mechanism' between the shear layer and compression/expansion wave system. Also, Zhuang *et al*[21] obtained a better match with the experimental result of Papamschou and Roshko[1] by employing the bounded two dimensional mode than the free three dimensional mode and concluded that confined shear layer is more unstable than the corresponding free shear layer. The wall effect was further analyzed by Morris *et al*[22] and Giridharan and Morris[23], this showed that except for certain specific duct shapes, the dominant supersonic instability waves are two dimensional and three dimensional modes are more rapidly damped as the flow convects and the shear layer thickness increases. Experimental investigations have not specifically elaborated on the wall effect which, as proposed by Tam and Hu[19], give rise to the new instability mechanism for confined supersonic mixing layer. Detailed measurements were not provided to explain whether the large scale structures originate from the supersonic instability mechanism, although many other important aspects were found and discussed. Two dimensional inviscid simulations of confined shear layer by Guirguis *et al*[16] and Faruk *et al*[17] exhibit well defined large structure, though not so organized, perhaps not so coherent as those found in the subsonic shear layer. Lu and Wu[18] have performed two dimensional simulation for mixing layer with a convective Mach number as high as 1·77 and shown that unless the supersonic mixing layer shocked down to subsonic speed range, 'Supersonic Instability' is fundamentally different from the subsonic Kelvin-Helmholtz instability and the duct walls play a vital role for generating the instability mechanism.

In the present work, as the shear layer is laterally confined, the role of large scale structure is very important in the evolution of the shear layer and can be understood from the two dimensional simulations.

Table 1
Inflow parameters for non-reacting shear layer

Species	u, (km/s)	T, (K)	M	p,(MPa)	Re/(mm)
H_2	2·4	103	3·09	0·021	1,600
N_2	3·8	2,344	3·99	0·021	22,000

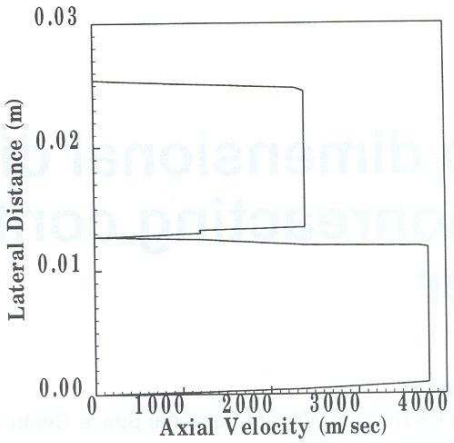

Figure 2. Velocity profile at the inflow plane (edge of splitter plate).

3.0 THE CODE AND COMPUTATIONAL DETAILS

The code used in the present calculations is the non-reacting version of SPARK2D code developed at the NASA LaRC by Drummond and Carpenter[24]. It discretises two dimensional Navier Stokes equations by using compact Mac-Cormack's scheme with fourth order spatial and second order temporal accuracy. This choice represents a compromise between the accuracy of higher order numerical algorithms and the robustness and efficiency of lower order methods. The code has been validated by computing a linearly unstable shear flow problem in the early stages of the growth. Carpenter and Kamath[25,26] have demonstrated that with the compact schemes considered here, the growth rates with the initial profiles based on the eigenfunctions predict those from linear stability theory for free shear layers to within 1% for a time duration equal to about five

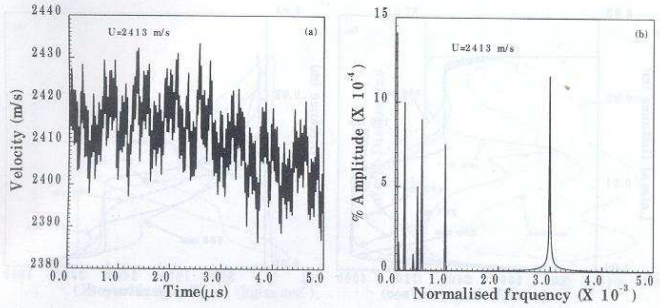

Figure 3. The imposed velocity fluctuations at the inflow plane (a) velocity *vs* time, (b) Fourier transform of velocity fluctuation.

times the sweep time of the flow field. This accuracy is adequate for the present computations needing a maximum of three sweep times – one sweep for clearing the flow field, and two more sweeps to collect statistical information and also check on the statistical invariance of the calculations.

The boundary conditions set for this problem are as follows. On the upper and lower solid boundary, no slip conditions for the velocities and the constancy of wall temperature are imposed.In the experimental investigation of hypervelocity mixing layer of Erdos *et al*[13], the primary stream is coming through a channel which has a constant area upstream of the splitter plate, while the secondary stream is formed by a contoured nozzle designed by the method of characteristics to produce a uniform Mach 3 stream at the exit plane as depicted in Fig 1. The initial boundary layer for the two streams are calculated from a laminar Navier Stokes solver based on Mac-cormack's predictor corrector explicit scheme. The initial velocity profile used in the present simulation is presented in Fig. 2.

In the mixing layer experiment of Erdos *et al*[13], the splitter plate which separates the two streams before entering the test section, has a thickness of 0·58mm. Accounting of this effect is important in the sense that the growth and the subsequent development of the mixing layer is dependent on the proper accounting of this finite thickness. No slip conditions for the velocities and the constancy of wall temperature are also applied in the portion of splitter plate thickness.

On the inflow stream is imposed velocity fluctuations over a range of frequencies at total rms intensity of 0·3% of the mean velocity as shown in Fig. 3, in which is shown velocity vs time plot in Fig. 3a and the normalized frequency vs amplitude plot in Fig. 3b. The frequency has been normalized with the mean velocity to channel width ratio. It can be seen that the input fluctuations have many components up to the normalized frequency of 0·003. The frequency range allows the mixing layer to grow as may happen in reality. The exit boundary condition is obtained by second order extrapolation and is considered satisfactory for this problem dominated by supersonic flow.

The flow domain is of size 535mm × 25.4mm. The two streams

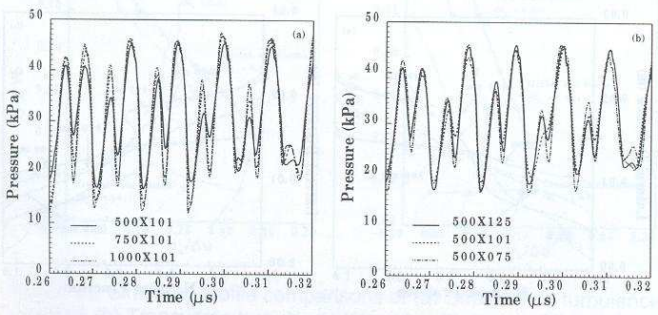

Figure 4. The pressure vs time obtained with grid refinements in (a) the axial direction, (b) the cross stream direction.

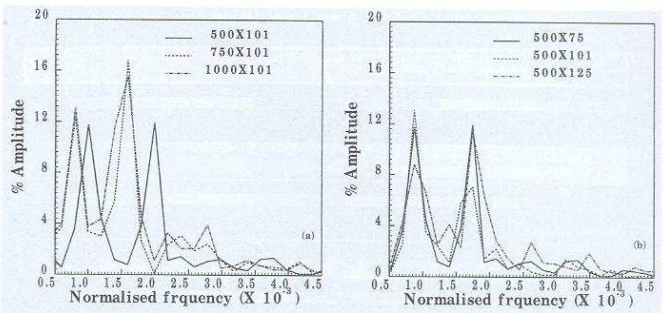

Figure 5. The spectral distribution of fluctuations on an amplitude vs normalised frequency plot (a) with grid refinements in the axial direction, (b) with grid refinements in the cross stream direction.

are separated by a splitter plate at a height of 12·7mm. The grid is stretched exponentially in the axial direction with minimum grid spacing is at the inflow boundary to capture the initial development of the mixing layer. In the lateral direction, minimum grid spacing is taken near the interface and it is stretched exponentially towards both the upper and lower wall. The wall boundary layer is resolved by taking very fine mesh near the solid wall and the grid is again stretched exponentially in the region away from the wall. The grid structure employed in the simulation has 1,000 points in the axial direction with minimum grid size of 0·3mm near the inflow plane and the maximum size of 0·8mm near the outflow boundary. In the lateral direction 101 grid points are employed with minimum grid spacing of 0·09mm near the interface and the maximum grid spacing is of order of 0·5mm in the region away from the mixing layer. The size of the minimum grid spacing near the solid wall is also taken as same as that of the interface. The grid considered in the simulation is sufficient to capture the large scale structure of the flow field as is evident from the grid resolution studies. Grid resolution calculations were made by varying the number of grids in both the axial and lateral directions. In this grid resolution study, five different grids namely, 1,000 × 101, 750 × 101, 500 × 101, 500 × 125 and 500 × 75 were used to determine the effect of grid resolution in the axial and cross-stream directions. The temporal variation of the pressure for grid refinement in the axial and cross-stream directions are presented in the Fig. 4. As can be seen, increasing the number of grids from 500 to 1,000 in the axial direction and from 75 to 125 in the cross-stream direction leave the results almost unchanged.

Further comparison on the effect of grid size on the spectral content of the pressure fluctuations are shown in Fig. 5 for axial and cross-stream grid refinements. The amplitudes are normalised by the mean and the frequency by the ratio of a characteristic thickness to mean velocity. The characteristic thickness is taken as the channel width. Even the spectral content of the fluctuations are well tracked except at high frequencies. Hence, the calculations are model free except at very small scales which are unlikely to affect the large scale structure of the flow. The grids chosen namely, 1,000 × 101 give good representation of the temporal evolution of the flow field. An additional feature of Fig. 5 is that the amplitude of fluctuations downstream goes up to 12-15%, where as the total rms inflow velocity fluctuations are only 0·3% of the mean, and the frequency content of the downstream fluctuations is much richer than in the inflow. Similar comparisons of velocity fluctuations downstream have shown similar good results for 1,000 × 101 grids. Hence it is concluded that the 1,000 × 101 grid chosen here is sufficient to give grid-independent solutions.

The computation continued for two sweeps till the solution attained statistical steady state. One sweep is taken as the time the flow takes to cross the test section length with its convective velocity. After the attainment of statistical steady state, various flow variables, like density and velocities are stored at all time steps over one sweep of calculation at all the lateral points over few sections of the

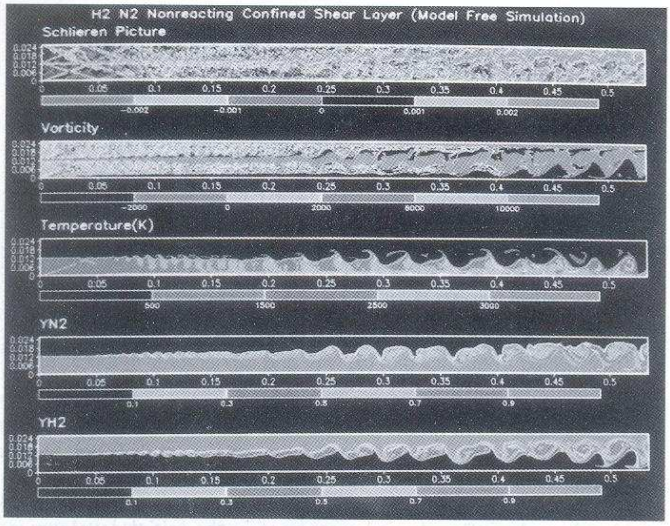

Figure 6. Contour plot of schlieren picture, vorticity, temperature, hydrogen and nitrogen mass fractions of confined mixing layer.

flow field. For calculating the turbulence quantities, the mean velocities were obtained by Favre averaging ($\tilde{u} = \overline{\rho u}/\overline{\rho}$, $\tilde{v} = \overline{\rho v}/\overline{\rho}$) and the mean density by conventional time averaging. The fluctuating quantities are the given by

$$u' = u - \tilde{u} \tag{1}$$

$$v' = v - \tilde{v} \tag{2}$$

The streamwise turbulence intensity (σ_u) and the transverse turbulence intensity (σ_v) is calculated from the stored transient data as:

$$\sigma_u = \frac{1}{n}\sqrt{\sum_{i=1}^{n}\overline{(u_i - \tilde{u})^2}} \tag{3}$$

$$\sigma_v = \frac{1}{n}\sqrt{\sum_{i=1}^{n}\overline{(v_i - \tilde{v})^2}} \tag{4}$$

4.0 RESULTS AND DISCUSSION

The instantaneous flow field for the non-reacting confined shear layer is presented through the contour plot in Fig. 6. The composite picture contains the contour plots of numerically generated schlieren picture, vorticity, temperature and the mass fraction of hydrogen and nitrogen in the whole flow domain. The shocks emanating from the splitter plate and from the edge of the boundary layer and their reflections from the wall is clearly visible. The shocks after undergoing various reflections and interactions develop complex flow features downstream. The growth of the mixing layer formed at the interface is clearly evident from the vorticity plot.

The upper stream of H_2 has a temperature of 103K and the lower stream of N_2 a temperature of 2,400K. Although the mixing of the two streams brings down the temperature of the hot gas considerably, there exists a higher temperature zone of more than 3,000K in the wall boundary layer of the lower stream. This feature of the mixing of the two streams will be further elucidated through the mean profiles of various parameters later. Hydrogen and nitrogen mass fraction contours are presented in the last two plots. The two streams although initially discrete, mix by turbulence and molecular diffusion. At the farthest downstream location the mixing is nearly complete.

For the calculation of the mean properties, the solutions are first allowed to attain statistical steady state. The transient surface pressures are stored at all axial points of the upper and lower walls at all time steps over one sweep of the calculation. Flow properties like velocities, pressure, density, temperature and mass fractions of the species hydrogen and nitrogen are also stored over one sweep at all lateral points at various axial locations. The mean properties of the flow variables are then obtained by averaging these transient data.

The comparisons of the computed mean surface pressures (both upper and lower walls) with the experimental result[13] are presented in Fig. 7. The computed surface pressure is very close to the experiment. For the upper wall from the location of 350mm from the splitter plate, the computed surface pressure is slightly above the experimental value. Considering the repeatability of the experimental data, the comparison can be considered reasonably good.

The mean profiles of the axial velocity and temperature at axial locations of 100mm, 200mm, 300mm, 400mm and 500mm are presented in Fig. 8. With the increase in the downstream distance, the smoothening of the velocity takes place with the decrease in the mean velocity in the lower stream and the increase in the velocity in the upper stream. The layer has grown more into the high speed (N_2) side as is clear from the unchanged profile region on the low speed

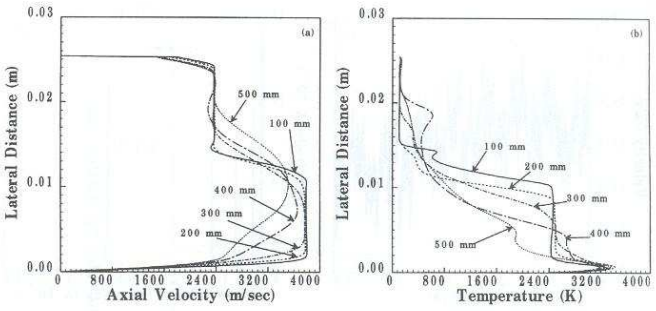

Figure 8. Mean profiles at various axial locations for $H_2 - N_2$ case. (a) Axial velocity, (b) temperature-confined mixing layer.

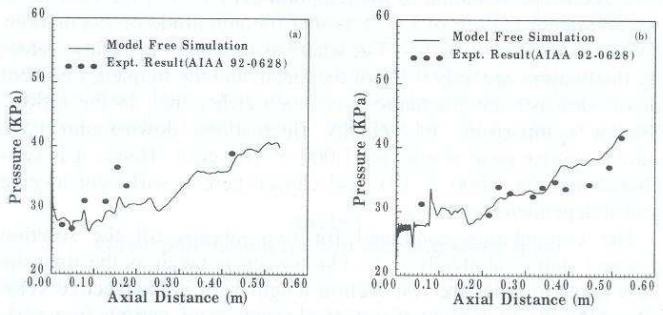

Figure 7. Surface pressure comparison between experiment and DNS results for $H_2 - N_2$ case. (a) Lower wall, (b) Upper wall.

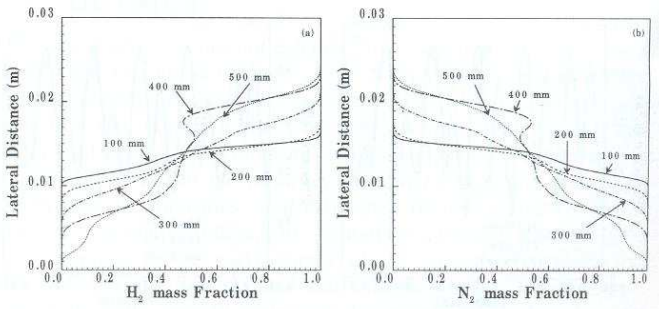

Figure 9. Mean profiles at various axial locations for $H_2 - N_2$ case. (a) H_2 mass fraction, (b) N_2 mass fraction – confined mixing layer.

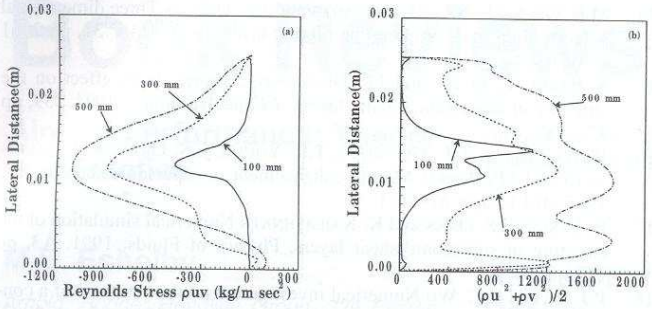

Figure 10. Profiles of the turbulent quantities at various axial locations for $H_2 - N_2$ case. (a) Reynolds Stress, (b) Turbulent kinetic energy – confined mixing layer.

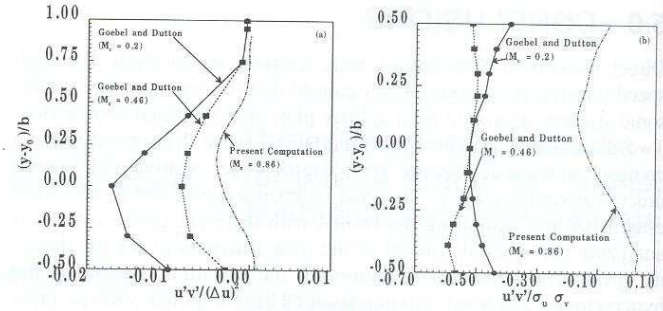

Figure 12. Similarity profile comparisons of (a) Kinematic Reynolds Stress, (b) Correlation coefficient of kinematic Reynolds Stress with those of Goebel and Dutton. (Experiments are for free shear layer and the computations are for confined shear layer.)

(H_2) side. This implies more of high speed fluid being found in the mixing layer, a feature described by Koochesfahani *et al*[27]. Although due to significant mixing between the hot and cold streams the temperature in the mixing layer is reducing continuously in the downstream locations, temperature in the lower boundary has exceeded 3,200K mainly due to viscous dissipation. The mean profiles of the H_2 and N_2 mass fraction are presented in Fig. 9. The molecular mixing between the two streams is clearly evident from the change of the mass fraction profiles.

The profiles of the turbulence quantities like Reynolds stresses and the turbulent kinetic energy have been derived from the stored time series data from the model free simulation and are presented in Fig. 10 at axial locations 100, 300 and 500mm. The value of Reynolds stress is negative and increases with distance from the splitter plate. Turbulent kinetic energy is also seen to increase in the flow direction. This indicates that energy is extracted from the mean flow and fed into the fluctuation field. This transfer of energy is mainly responsible for the sustenance of turbulence as the shear layer evolves. The turbulence level in the mixing layer is much larger in comparison to the turbulence level in the wall boundary layer. One can also notice from the profiles that the Reynolds stress is almost insignificant in the boundary layers except near the far downstream location of the lower wall, where a small positive value indicates to the presence of countergradient effect.

Similarity profiles of various turbulent quantities namely streamwise and transverse turbulent intensities, anisotropy, kinematic Reynolds stresses and the correlation coefficients of the kinematic Reynolds stresses are computed from the stored transient data of the Direct numerical simulation. The quantity $\eta = (y - y_0)/b$ is chosen as the similarity parameter, where b is the shear layer thickness defined as the distance between the transverse locations where the value of $|(u - u_a)/(u_a - u_b)|$ is 0.9 and 0.1, u_a and u_b are the velocities of the upper and lower streams. The mixing layer centreline y_0 is taken as the midpoint between the transverse locations where the value of $|(u - u_a)/(u_a - u_b)|$ is 0·9 and 0·1. The turbulent intensities are normalized by Δu – the velocity difference between the upper and lower streams. The kinematic Reynolds stress is normalized by Δu^2. The turbulent intensities are compared with the results of Goebel and Dutton Experiment[3] in Fig. 11. *It must be noted that the present computations are for confined mixing layer with high convective Mach number compared to the experiment of Goebel and Dutton where a free shear layer is studied at lower convective Mach numbers.* As no turbulence measurements are available for the supersonic confined mixing layer, the comparisons can help us to assess the qualitative nature of the turbulent statistics for the confined shear layer. There is a reduction in the turbulence intensities (both streamwise and transverse) with increase in convective Mach numbers in the region of the mixing layer. This is in conformity with the results of other studies of the free shear layer. The shape of the profile of streamwise turbulent intensity in the present computation is different from that of the Goebel and Dutton mainly due to the presence of the counter- gradient effect present in the downstream portion of lower wall boundary layer. The similarity profiles of the kinematic Reynolds stress and the correlation coefficients of the kinematic Reynolds stress are compared in Fig. 12. Reynolds stress shows decreasing trend with increasing convective Mach number and the correlation coefficient for the present computation is also much smaller compared to the Goebel and Dutton experiment. The anisotropy (σ_u/σ_v) profiles presented in Fig. 13 are markedly different for the present case, particularly in the wall boundary layer region.

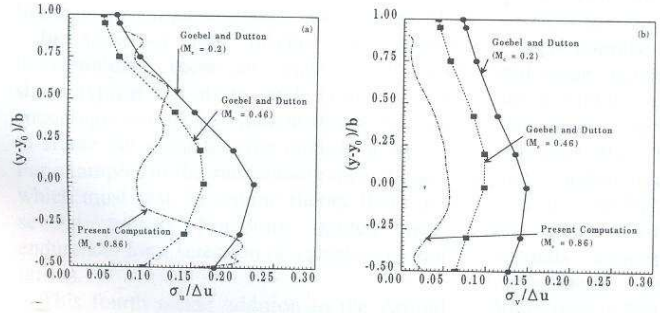

Figure 11. Similarity profile comparisons of (a) Streamwise turbulence intensity, (b) Transverse turbulence intensity with those of Goebel and Dutton. (Experiments are for free shear layer and the computations are for confined shear layer.)

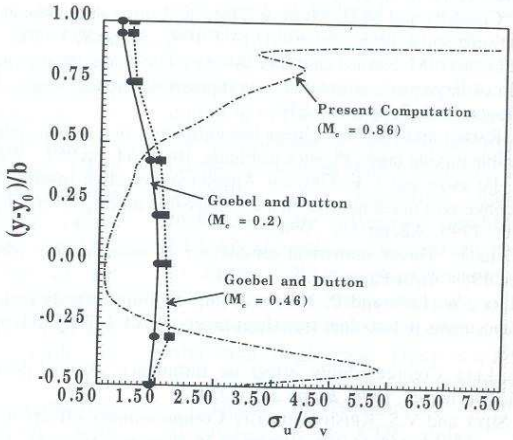

Figure 13. Similarity profile comparisons of anisotropy with those of Goebel and Dutton. (Experiments are for free shear layer and the computations are for confined shear layer.)

5.0 CONCLUSIONS

Direct Numerical Simulations were carried out to study the high speed non-reacting mixing layer caused due to mixing of two supersonic streams separated by a splitter plate in a confined test section. Two dimensional Navier Stokes equations were discretised using a compact numerical scheme with fourth order spatial and second order temporal accuracy. The grid independence of the results were established by comparing the results with different grids, as well as analyzing the spectral content of the flow fluctuations for the different grids. The simulation captures all the essential features of the hypervelocity confined mixing layer. The computed surface pressures for both lower and upper walls match fairly well with the experimental results. The examination of contour plots and the mean properties of the flow indicate that the growth of the mixing layer is towards the high speed side of the flow because of more entrainment by the high speed flow.

Various turbulence quantities were estimated from the stored time series data of the DNS calculation. In the absence of any measurements of turbulence quantities for high speed confined mixing layer, the turbulence quantities were compared with the experimental values of the free supersonic mixing layers. The general features of the turbulence quantities of the free shear layer is also observed in the confined mixing layer. The Reynolds stress, streamwise and transverse turbulence intensities are seen to be less for higher convective Mach number. The Reynolds stress profile indicate the presence of counter gradient effect in the far downstream position of the lower wall boundary layer, although it is almost negligible in the major portion of the wall boundary layer.

ACKNOWLEDGMENT

The authors would like to express their sincere thanks to Dr V. Adimurthy of VSSC, Thiruvananthapuram for the support provided for carrying out this work.

REFERENCES

1. D. PAPAMSCHOU and A. ROSHKO The compressible turbulent shear layer :an experimental study, *J Fluid Mechanics*, 1988. **197**, pp 453 – 457.
2. M. SAMINY and G.S. ELLIOT Effect of compressibility on the characteristics of free shear layers, *AIAA J* 1990. **28,** pp 439-445.
3. S.G. GOEBEL and J.C. DUTTON Experimental study of compressible turbulent mixing layers, *AIAA J* 1991. **29**, pp 538 – 546
4. J.L. HALL Experimental investigation of structure, mixing and combustion in compressible turbulent shear layers, PhD Thesis, California Institute of Technology 1991.
5. N.T. CLEMENS and M.G. MUNGAL Two and three dimensional effects in the supersonic mixing layers, *AIAA J* 1992. **30,** pp 973 – 981.
6. G.S. ELLIOTT, M. SAMINY and S.A. ARNETT The characteristics and evolution of large scale structures in compressible mixing layers, Physics of Fluids, 1995. **7,** pp 864 – 876.
7. S.A. RAGAB and J.L. WU Linear instabilities in two dimensional compressible mixing layer, Physics of Fluids, 1989. **A1,** pp 957 – 966.
8. T.L. JACKSON and C.E. GROSCH Absolute/convective instabilities and the convective mach number in a compressible mixing layer, Physics of Fluids, 1990. **A2,** pp 949 – 954.
9. S.K. LELE Direct numerical simulation of compressible free shear layer, 1989. *AIAA* Paper No. 89 – 0374.
10. T. LIOU, W. LIEN and P. HUANG Compressibility effects and mixing enhancements in turbulent free shear layers, *AIAA J* 1995. **33,** pp 2332-2338.
11. S.K. LELE Compressibility effect on turbulence, Annual Review of Fluid Mechanics, 1994. **26,** pp 211 – 254.
12. W. SHYY and V.S. KRISHNAMURTHY Compressibility effects in modeling complex turbulent flows, Progress in aerospace sciences, 1997. **33,** pp 587 – 645.
13. J. ERDOS, J. TAMAGNO, R. BAKOS and R. TRUCCO Experiments on shear layer mixing at hypervelocity conditions, 1992. *AIAA*-92-0628.
14. M.R. GRUBBER, N.L. MESSERSMITH and J.C. DUTTON Three dimensional velocity field in a compressible mixing layer, 1993. *AIAA* **31,** pp 2061 – 2067.
15. S. BARRE, C. QUINE and J.P. DUSSAUGE Compressibility effect on the structure of supersonic mixing layers, *J Fluid Mechanics*, 1994. **259,** pp 47 – 78.
16. R.H. GUIRGUIS, F.F. GRINSTEIN, T.R. YOUNG, E.S. ORAN, K. KAILASHNATH and J.P. BORRIS Mixing enhancement in supersonic shear layers, 1987. *AIAA* Paper 87-0373.
17. B. FARUK, E.S. ORAN and K. KAILASHNATH Numerical simulation of the structure of supersonic shear layers, Physics of Fluids, 1991. **A3,** pp 2786-2798.
18. P.J. LU and K.C. WU Numerical investigation on the structure of a confined supersonic mixing layer, Physics of Fluids, 1991 **A3,** pp 3063-3069.
19. C.K.W. TAM and F.Q. HU The instability and acoustic wave modes of supersonic mixing layer inside a rectangular channel, *J Fluid Mechanics*, 1989. **203,** pp 51-76.
20. J.A. GREENGOUGH, J.J. RILEY, M. SOETRISNO and D.S. EBERHARDT The effect of walls on a compressible mixing layer, 1989. *AIAA* Paper 89-0372.
21. M. ZHUANG, P.E. DIMOTAKIS and TOSHI KUBOTA The effect of walls on a spatially growing supersonic shear layer, Physics of Fluids, 1990. **A2,** pp 599-604.
22. P.J. MORRIS, M.G. GIRIDHARAN and K. VISWANATHAN Turbulent mixing in plane and axisymmetric shear layer, 1990. *AIAA* Paper 90-0708.
23. M.G. GIRIDHARAN and P.J. MORRIS The development of wave packets in supersonic shear layer, 1991. *AIAA* Paper 91-0626.
24. J. P. DRUMMOND Supersonic reacting internal flow field, in Numerical Approaches in Combustion Modeling edited by E.S. Oran and J.P. Borris, *Progress in Aeronautics and Astronautics*, 1991. **135,** pp 365-420.
25. M.H. CARPENTER and H.KAMATH Three dimensional extension to the SPARK combustion code NASA-Langley, 1988. NASA-CP-5029, pp 107-137.
26. M.H. CARPENTER A generalized chemistry version of SPARK 1998. NASA-CR-4196
27. M.M. KOOCHESFAHANI, P.E. DIMOTAKIS, and J.E. BROADWELL A 'Flip' experiment in a chemically reacting turbulent mixing layer, *AIAA* 1985. **23,** ~pp 1191.